Kinetic lattice-gas model of cage effects in high-density liquids and a test of mode-coupling theory of the ideal-glass transition

Walter Kob * and Hans C. Andersen†
Department of Chemistry, Stanford University, Stanford, California 94305
(Received 25 June 1993)

We have devised a kinetic lattice-gas model of an atomic liquid that incorporates the physical features associated with the formation of cages around a particle at high density. The model has simple equilibrium statistics, with a maximum of one particle per lattice site, and simple dynamical rules, so that it is feasible to perform dynamical calculations of the fluctuations about equilibrium over very long time scales. The cages inhibit the motion of the particles and cause the self-diffusion coefficient to fall rapidly with increasing density. Simulation results indicate that as the density ρ, defined as the number of particles per lattice site, approaches 0.881, the self-diffusion constant behaves in a critical way as $(0.881-\rho)^{3.2}$. The time dependence of density-density correlation functions is calculated from the simulation results, and relaxation times extracted from these functions show a similar critical behavior. These results suggest that the model undergoes a dynamical transition from ergodic to nonergodic behavior. By investigating different system sizes we exclude the possibility that the observed transition is just a finite-size effect related to the bootstrap percolation problem. The mode-coupling theory (MCT) of ergodic-nonergodic transitions in the absence of activated hopping processes is tested for this model by comparing the behavior of the density correlation functions with the predictions of MCT. Surprisingly few of the MCT predictions hold for the system, despite the fact that the model was devised to incorporate, in a schematic way, the dynamical cage effects that the MCT is usually regarded as describing. Thus the MCT does not provide a correct description of the cage-induced ideal-glass transition of this model.

PACS number(s): 61.20.Ja, 64.70.Pf, 51.10.+y, 05.20.−y

I. INTRODUCTION

Over the last ten years there has been an impressive development in our understanding of supercooled liquids in the vicinity of the glass transition. Advances were made through novel experimental techniques and the development of new theories that describe such systems. The most outstanding example of these theories is the so-called mode-coupling theory (MCT) proposed by Bengtzelius, Götze, and Sjölander and, independently, by Leutheusser [1] and developed further mainly by Götze and Sjögren [2–5]. Although originally developed to describe the dynamics of simple liquids it was found that the applicability of the theory is much wider. It can, for example, also be used to interpret the dynamical behavior of materials as complex as polymers [5]. Despite this broad applicability it is unfortunately still not possible to say *a priori* whether or not the dynamical behavior of a given system should be correctly described by MCT or not. Therefore investigations to increase our understanding on this point are certainly most useful.

The version of MCT proposed by Bengtzelius *et al.* and by Leutheusser takes into account only certain types of terms of a more general theory whose origin is the kinetic theory of simple liquids [6]. The terms that are included give closed equations of motion for the spatial Fourier transform of the density-density autocorrelation function. These equations are regarded as describing the motion of particles in the cages formed by surrounding particles [5,7]. This motion is clearly cooperative, since a single particle can move an appreciable distance only if its cage is disrupted, and the disruption of a cage can occur only if the cage particles themselves can move. At this level of approximation MCT predicts the possibility of a structural arrest at high density or low temperature, i.e., when the cooperative relaxation of the cages is impossible. Taken at face value, such an arrest would be an ergodic-nonergodic transition or an idealized glass transition.

The terms that are neglected in this simplest version of the theory are those that couple the density-density autocorrelation function to the particle current-current autocorrelation function. These terms are regarded as describing activated processes whose rates are very low at low temperature but which nevertheless are capable of relaxing the system to equilibrium for very long times. If the coupling to the currents is taken into account the theoretical picture that emerges becomes quite a bit more complicated in that the sharp transition predicted by the simpler theory becomes washed out, i.e., ergodicity is restored even at low temperatures, and new time scales arise [4]. However, it has been found that most of the main features of the idealized glass transition are still present and this justifies the comparison of the simple theory with experiments and the results of the computer simulations [8–10].

As noted above, the MCT has been compared with

*Electronic mail: kob@d31ha1.stanford.edu
Present address: Institut für Physik, Johannes Gutenberg-Universität, Staudingen Weg 7, D-6500 Mainz, Federal Republic of Germany.
†Electronic mail: fb.hca@forsythe.stanford.edu

data on experimental systems that are considerably more complex than the simple liquids for which the theory was originally developed. The success of MCT in describing such data is confirmation of the very reasonable idea that even for very complicated materials cages can cause structural arrest and activated processes can restore ergodicity. Presumably the mathematical structure of MCT is capable of providing a quantitative description of these effects for more complicated materials as well as for atomic liquids. MCT in fact predicts the existence of several universality classes of dynamic transitions and therefore provides a rationale for the possibility that very different materials might have transitions with similar mathematical properties.

In a recent paper we have compared the predictions of MCT with computer simulation data for a kinetic lattice model of dense fluids [10]. The model described the motion of particles on a lattice and included short-ranged attractive and repulsive interactions between particles. Because it was a lattice model with very simple dynamics, we were able to equilibrate the system at lower temperatures and calculate correlation functions for longer times than would have been feasible for an analogous continuum material. While many of the predictions of the simple MCT were found to be valid for this system, others were found not to be in agreement with the simulation results. It is difficult to tell whether the limited success of the theory is evidence that the theory is fundamentally incorrect for this model or whether the lattice model under consideration is one for which activated processes must be taken into account for an adequate description. A similar uncertainty arises when the theory is compared with experimental data.

We decided to study in more detail the question of whether and how cage effects can cause structural arrest at high densities and whether the simple mode-coupling theory description of this arrest is correct. In order to do so, we have devised a kinetic lattice model whose dynamics contains nothing more than the physics of the cage effect with no possibility of activated hopping processes. This is the topic of the present paper. Our goal was to simulate the model to determine if at high density it would undergo an ergodic-nonergodic transition. Moreover, the model can easily be modified to include activated processes, and thus we hoped that this would provide a useful and less ambiguous basis for testing both the simple MCT and its extensions.

There have been several previous investigations of lattice models to study ergodic-nonergodic transitions, sometimes also called dynamical phase transitions, and their connection to the glass transition. To the best of our knowledge the first attempt to investigate such a system is due to Fredrickson and Andersen, who proposed the facilitated kinetic Ising model and developed an approximate theory that predicted such a transition for this model [11]. However, subsequent numerical simulations showed that there is increasingly sluggish behavior but no sharp transition as the temperature is lowered [12]. Ertel *et al.* investigated the dynamics of a two dimensional hard square lattice gas [13]. Computing the self-diffusion coefficient they found a dynamical transition, but concluded that this singularity will vanish in the thermodynamic limit. Froböse and Jäckle *et al.* investigated this point further and found a strong dependence of the diffusion constant on the system size [14,15]. Jäckle *et al.* also pointed out that there is a connection between the dynamics of these kinds of systems and the so-called bootstrap percolation problem. We will elaborate on this point in Sec. V. By means of computer simulations Reiter *et al.* [16] then investigated the dynamics of two kinetic Ising models whose corresponding cellular automata show a transition even in the thermodynamic limit [17]. However, these authors did not compare their results with the predictions of MCT and presented mainly qualitative results. Most recently Jäckle and Sappelt tried to test the applicability of MCT to the models investigated in Ref. [16] and found that one possible way to do the mode-coupling approximations leads to unphysical results [18]. In addition they showed that an approximation scheme they called the effective-medium approximation is able to reproduce the transition in a qualitative way. However, quantitatively this kind of approximation does not seem to be very accurate and it remains to be seen whether this theory can be improved.

The outline of the rest of the paper is as follows. In Sec. II we give a short introduction to MCT and compile the essential formulas for this work. In Sec. III we introduce our model and give some of the details of our simulations. Section IV is devoted to the presentation of the results. In Sec. V we discuss these results and some finite size effects of the system. Finally, Sec. VI contains a summary of our findings and our conclusions on this work.

II. MODE-COUPLING THEORY

In this section we give a short introduction to the essentials of MCT and compile some of the predictions of the theory, the derivations of which can be found in the original papers. A much more extensive discussion of the theory can be found in the the review articles by Götze, Götze and Sjögren, and Schilling [19].

Mode-coupling theory is a mathematical framework developed to describe the dynamical behavior of supercooled liquids. The theory makes detailed predictions of the way correlation functions behave in the vicinity of the glass transition. The main focus of MCT is the correlator $\Phi(\mathbf{q},t)$ obtained by normalizing the intermediate scattering function $F(\mathbf{q},t) = \langle \delta\rho_{\mathbf{q}}(t)\delta\rho_{-\mathbf{q}}(0)\rangle$ by the static structure factor $S(\mathbf{q}) = \langle \delta\rho_{\mathbf{q}}\delta\rho_{-\mathbf{q}}\rangle$. Here $\delta\rho_{\mathbf{q}}(t)$ is the fluctuation of the density for wave vector $\mathbf{q}$ at time t and $\langle\,\rangle$ denotes the average over the canonical ensemble. Equations of motion, called mode-coupling equations, can be derived for $\Phi(\mathbf{q},t)$ and, under certain approximations, solved. These equations depend parametrically on $S(\mathbf{q})$ and therefore on temperature and density. It is found that for high temperatures (or low densities) $\Phi(\mathbf{q},t)$ decays to zero in the long-time limit. Therefore the system is said to be ergodic. However, if the temperature is below a certain critical temperature T_c (or the density above a critical density ρ_c) this is no longer true. In this case the infinite time limit of $\Phi(\mathbf{q},t)$ is

given by a nonzero constant. The system has therefore undergone a structural arrest and hence is no longer ergodic. Note that similar statements can be made for the correlator $\Phi_s(\mathbf{q},t)$ that is given by substituting the self part of the intermediate scattering function, $F_s(\mathbf{q},t)$, for the intermediate scattering function $F(\mathbf{q},t)$. In fact MCT predicts much more generally that the statements hold for all correlators Φ_{XY} between quantities X and Y for which $\langle X\delta\rho_{\mathbf{q}}\rangle$ and $\langle Y\delta\rho_{\mathbf{q}}\rangle$ do not vanish. It has to be emphasized that the transition presented above happens only if the activated hopping processes, mentioned in the Introduction, are neglected. In the following we will also restrict our discussion to the type of singularity commonly called a B transition [19]. This is the type of transition that is used to describe the liquid to glass transition for fluids.

Before we present the predictions of MCT for the dynamical behavior of the correlators in the vicinity of the glass transition it is useful to introduce two quantities: the separation parameter ϵ and the so-called exponent parameter λ. ϵ is a dimensionless distance from the critical point and is defined as $\epsilon \equiv (T_c - T)/T_c$ [or $\epsilon \equiv (\rho - \rho_c)/\rho_c$]. The exponent parameter λ is a system dependent number and satisfies the inequalities $0 < \lambda < 1$. It can be calculated if the form of the equations of motion is known.

By a careful analysis of the time dependence of $\Phi(\mathbf{q},t)$ and $\Phi_s(\mathbf{q},t)$, obtained from the solutions of the mode-coupling equations in the limit of $\epsilon \to 0$, the following properties of the system can be shown to hold. (Note that in order to simplify the discussion we will state all the results for the case in which the temperature is the thermodynamic variable which drives the transition. However, all the results remain unchanged if this variable is the density.)

(i) The diffusion constant. The constant of diffusion D shows for $\epsilon < 0$ (i.e., on the liquid side of the transition) the critical behavior

$$D \propto |\epsilon|^{\gamma}. \tag{1}$$

The exponent γ is given by

$$\gamma = \frac{1}{2a} + \frac{1}{2b}, \tag{2}$$

where a and b are the unique solutions of the equations

$$\frac{\Gamma(1-a)^2}{\Gamma(1-2a)} = \frac{\Gamma(1+b)^2}{\Gamma(1+2b)} = \lambda. \tag{3}$$

Here $\Gamma(x)$ stands for the Γ function. Since a and b depend on λ, the exponent γ will depend on λ too and therefore is not a universal quantity. It can be shown that $0 < a < 1/2$ and $b > 0$. Therefore $\gamma > 1$ holds as well.

(ii) Long-time relaxation behavior. For long times the correlators $\Phi_{XY}(t)$ are well approximated by a Kohlrausch-Williams-Watt (KWW) law, i.e.,

$$\Phi_{XY}(t) \cong A\exp[-(t/\tau)^{\beta}]. \tag{4}$$

The stretching (or Kohlrausch) exponent β is independent of temperature. Since the prefactor A shows only a weak dependence on temperature the main temperature dependence of Φ_{XY} stems from the relaxation time τ which, like the diffusion constant, shows a power-law behavior. The exponent of this power law is given again by γ [see Eq. (2)]. Since neither β nor A shows a pronounced temperature dependence a plot of correlators corresponding to different temperatures versus $t/\tau(T)$ will show that for long times all these curves collapse onto a master curve. Therefore this phenomenon is called the time-temperature superposition principle.

(iii) Intermediate-time relaxation behavior. For times between the microscopic times and the times for which (4) holds, the so-called β-relaxation regime, the correlators can be written in the following form:

$$\Phi_{XY}(t) = f + h\sqrt{|\epsilon|}g_{\pm}(\hat{t}), \qquad \text{with} \quad \hat{t} = t|\epsilon|^{1/2a}/t_0. \tag{5}$$

Here $\pm$ stands for the glass and liquid side of the transition, respectively, and t_0 is a microscopic time. The constant f, called the nonergodicity parameter, is identified as the effective Debye-Waller factor when $\Phi_{XY} = \Phi$ and as the effective Lamb-Mössbauer factor when $\Phi_{XY} = \Phi_s$. The amplitude factor h depends on the quantity investigated but not on temperature. The most important feature of Eq. (5) is that the temperature enters the expression only by the square root of ϵ and through the rescaled time $\hat{t}$. In other words, the master functions $g_{\pm}$ are independent of temperature and of the quantity investigated. For $\hat{t} \ll 1$ they are given by

$$g_{\pm} \propto \hat{t}^{-a}. \tag{6}$$

For $\hat{t} \gg 1$ the behavior on the liquid side ($\epsilon < 0$) and that on the glass side ($\epsilon > 0$) are very different. For $\epsilon > 0$ one finds

$$g_{+}(\hat{t}) \to 1/\sqrt{1-\lambda} \quad , \tag{7}$$

i.e., the correlator does not decay to zero for long times, and for $\epsilon < 0$

$$g_{-}(\hat{t}) = -B\hat{t}^{b}, \qquad \text{with} \quad B > 0. \tag{8}$$

The power law given by Eq. (8) is called the von Schweidler law and holds only for times such that $h\sqrt{\epsilon}g_{-}(\hat{t})$ is small compared to one. It should be noted that constants a and b appearing in Eqs. (5), (6), and (8) are the same as those in Eq. (2) which shows the intimate connection proposed by MCT between the β-relaxation regime and the long-time behavior of the correlators.

III. MODEL AND DETAILS OF THE SIMULATIONS

In this section we introduce our model and give some of the details of our simulations.

The main goal of this work is to investigate the applicability of the MCT of the idealized glass transition to a system that shows the effect of cage formation at high densities but that has no activated processes. We also wanted to construct a lattice model for which the number of particles is locally conserved, in contrast to the kinetic Ising models previously devised to study ergodic-

nonergodic transitions, for which the z component of the spin is not conserved.

Our system is a lattice gas of N classical particles. The positions of the particles are discrete and are given by the sets of vertices, or lattice sites, of a simple-cubic lattice, i.e., the position of the ith particle ($i \in \{1, \ldots, N\}$) is given by $\mathbf{R}_i$ where $\mathbf{R}_i \in \mathbb{Z}^3$. For convenience we have assumed that the lattice spacing is one. Each particle occupies exactly one vertex and each vertex can be occupied by at most one particle. Apart from this hard core interaction there are no other interactions between the particles. There are V ($= L^3$) lattice sites, and the system is a cubic array of such sites of length L. All configurations of N particles on V vertices in which no two particles occupy the same site have the same energy and the same weight in the equilibrium ensemble of states. This feature simplifies the numerical simulation significantly since no equilibration of the system is needed. Thus one can generate an initial configuration by distributing the N particles randomly onto the lattice, and start the dynamics and the collection of the results immediately. This feature allows us to investigate time scales which are significantly larger than those attainable for systems that require equilibration. We imposed periodic boundary conditions on the finite-sized system, which play no role for the equilibrium properties of the model but which will be important for the dynamics.

The dynamics of the particles is given by the following algorithm. (1) Pick a particle at random (say particle j). Then randomly pick one of the six nearest neighbor sites of $\mathbf{R}_j$. Let the position of this site be $\mathbf{R}_j + \mathbf{d}$, where $\mathbf{d}$ is a unit vector. (2) Test whether the following three conditions are fulfilled. (i) Position $\mathbf{R}_j + \mathbf{d}$ is not occupied by another particle. (ii) Position $\mathbf{R}_j$ has m or fewer occupied nearest neighbor sites (i.e., particle j has m or fewer nearest neighbor particles). (iii) Position $\mathbf{R}_j + \mathbf{d}$ has $m+1$ or fewer occupied nearest neighbor sites (i.e., particle j if moved to this site would have m or fewer nearest neighbor particles). If these three conditions are fulfilled move particle j from position $\mathbf{R}_j$ to position $\mathbf{R}_j + \mathbf{d}$, advance the clock by $1/N$th of a time unit and go to (1). (3) If one or more of the conditions in (2) is not fulfilled, leave the position of particle j unchanged, advance the clock by $1/N$th of a time unit, and go to (1).

We now address the choice of m. For any choice of m, this algorithm satisfies the detailed balance condition for the equilibrium ensemble. [For this ensemble, all allowed states have the same weight, and so the detailed balance condition reduces to the following requirements: (1) it should be impossible to make a transition from an allowed state to a forbidden state; (2) if a transition from one allowed state to another is possible, then the reverse transition should have the same transition probability. It is easily verified that these two requirements are satisfied by this algorithm.] If the value of m is as large as 5 (i.e., if particles with as many as five neighbors were able to move), then restrictions (ii) and (iii) would impose no additional restrictions beyond that specified in (i). The model would incorporate none of the physics of a cage effect and would clearly be ergodic at all densities. The dynamics of such a model has been investigated by Ajay and Palmer [20]. On the other hand, if m were as small as 2, then the system would not be ergodic even at low densities. (To see this, consider a configuration in which eight particles are arranged in the form of a cube. Such configurations have a nonzero weight at low densities, but none of the particles would be capable of moving since each has three nearest neighbors. This immobility would persist for all times and the system would not be ergodic.) We want to choose m to be as small as possible, in order to ensure that the dynamics becomes sluggish at high density, while still allowing the system to be ergodic at low density. Accordingly we chose m to be 3. Although we do not have a proof that the dynamics at low density is really ergodic for this value of m we have not found any configurations at low densities that have a nonzero measure and that lead to nonergodic behavior. In addition, our simulations indicate that the system is ergodic at low densities.

To conclude this section we give some of the details of our simulations. The system sizes we investigated were $L = 10, 14$, and 20. We covered densities between 0.1 and 0.86, which corresponds to (for the largest system) 800 particles at the lowest density and 6880 particles at the highest density. The length of the runs was between 100 SPP (steps per particle) at low densities and 5×10^6 SPP at high densities. We averaged over typically 2000 initial configurations at low densities and about 100 configurations at high densities. A time of one SPP corresponds roughly to the time it takes for an atom in a dense liquid to vibrate in its cage. If we identify this with approximately 0.1 ps for an atomic liquid, then the longest of our calculations corresponds to a physical time of the order of 0.5 μs, which is much longer than can routinely be achieved in computer simulation of continuum fluids, and this calculation was repeated 100 times with different initial conditions.

For densities up to about 0.82 the numerical implementation of the algorithm was exactly as we described it at the beginning of this section. However, for high densities such an implementation is not very efficient since too many moves are rejected. We therefore used an algorithm that is exactly equivalent to the one described above but that is much more efficient at high densities. In this new algorithm one selects from only those particles that are actually movable and advances the clock in a compensatory manner. Similar ideas have been proposed elsewhere (see, e.g., [12]). The computational overhead for keeping track of which particles are movable is quite large but independent of density. Hence this kind of algorithm only becomes efficient at sufficiently high densities. We found that this second algorithm is faster than the first one for densities above 0.82.

IV. RESULTS

This section is devoted to the presentation of the results of our simulations. The first subsection deals with the diffusion constant and the second subsection with density-density correlation functions. Note that most of

the figures presented here are for the largest system we investigated ($L = 20$) since it was for this system size that the effects presented here were most pronounced. However, all the effects have also been found for the smaller systems. All results are reported in units of one lattice spacing and in units of SPP.

A. Diffusion constant

In order to determine whether a given system has a dynamical transition it is useful to determine the diffusion constant of the particles. We therefore determined the self-diffusion constant by monitoring the mean-squared (MS) displacement of the particles as a function of time. In Fig. 1 we show this quantity in a double logarithmic plot. Thus straight lines correspond to power-law behavior. We plot the data for all densities and system sizes investigated (see figure caption for details). Note that for computational efficiency we calculated the MS displacement (as well as the correlation functions discussed later) for different time windows, each having a width of two decades and sampling a different part of phase space. The fact that curves stemming from different windows almost coincide at those times where the windows overlap gives an estimate for the accuracy of the data.

For low densities ($\rho \leq 0.3$) the curves for the three different system sizes are indistinguishable and have unit slope, which corresponds to normal diffusion. For higher densities the curves start out with a slope which is less than one and the slopes become one only for long times. For densities above 0.75 the size dependence of the curves becomes noticeable. We find that the curves for the larger L's are higher than those for the smaller L's. We will comment on this observation in Sec. V. In order to determine the diffusion constant D we have fitted the asymptotic (i.e., long-time) behavior of the MS displacement curves to a straight line with unit slope. D can then easily be read off from this straight line as its value at time $t = 1$.

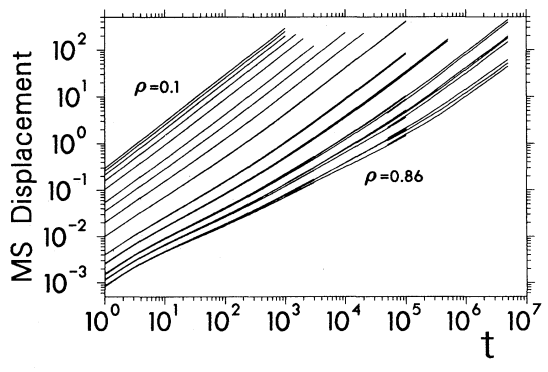

FIG. 1. Mean-square displacement for all densities and system sizes ($L = 10$, 14, 20) investigated. Densities from top left to bottom right: 0.1, 0.2, 0.3, 0.4, 0.5, 0.6, 0.65, 0.7, 0.75, 0.8, 0.82, 0.84, 0.85, 0.86. For a given density the lowest curve is for $L = 10$ and the top curve for $L = 20$.

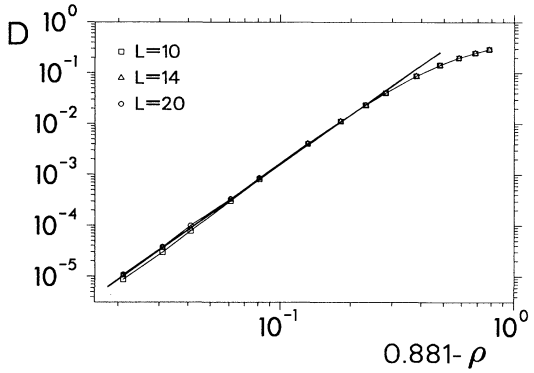

FIG. 2. Diffusion constant D for $L = 10$, 14, and 20 versus $0.881 - \rho$. The straight line is a power-law fit with exponent 3.1.

In Fig. 2 we plot the diffusion constant D versus $0.881-\rho$. The constant 0.881 was determined by a power-law fit to the data at high densities and the figure shows that this fit is clearly convincing since it fits the data well for over three decades of D. In doing the fit we have concentrated on the data of the two larger systems. For the exponent γ of the power law we find 3.1, which compares well with values found for other types of glassy systems [9]. If we make separate fits to the three individual data sets we find the critical densities to be 0.882, 0.882, and 0.881 for $L = 10$, 14, and 20, respectively. These figures have an error of about 0.002 and are therefore compatible with a single value of the critical density. Thus we can conclude from this plot that the dynamics of the system shows a singular behavior at about $\rho = 0.881$. We also tried to fit the data with the often employed Vogel-Fulcher law, $D \propto \exp[B/(\rho_c - \rho)]$. Note that if the range of ρ (or T, respectively) of the data are not large enough it is often quite difficult to determine whether the data are fitted better by a power law or by a Vogel-Fulcher law. The reason for this is the so-called "Bardeen identity" which says that for small ranges of ρ a power law can be very well approximated by a Vogel-Fulcher law[21]. However, for our case we found that our data are precise enough and the range in ρ sufficiently large, to exclude the possibility of a Vogel-Fulcher law. Thus the singular behavior of D is in accordance with the prediction of MCT.

B. Density-density correlation functions

We now turn our attention to time dependent correlation functions. For systems with a continuous symmetry of space it is usually customary to investigate the van Hove correlation function $G(\mathbf{r}, t)$ [22]. For isotropic systems $G(\mathbf{r}, t)$ depends only on the magnitude of $\mathbf{r}$ and therefore one can integrate over the angular dependence of $\mathbf{r}$. For a system with a discrete symmetry of space this is not possible and we therefore define the following autocorrelation function:

$$G_{s1}(r,t) = \frac{1}{3N}\sum_{\alpha}\sum_{i=1}^{N}\langle\delta(r_i^{\alpha}(t) - r_i^{\alpha}(0) - r)\rangle - \frac{1}{L}. \quad (9)$$

Here $r_i^{\alpha}(t)$ denotes the α component of the position of particle i at time t. Thus the sum on the right hand side of Eq. (9) is the probability at time t of finding a particle in a plane that is r lattice spacings away from the plane it started in at time zero. From this probability we subtract $1/L$, the long-time limit of this probability, so that $G_{s1}(r,t)$ goes to zero for long times. From $G_{s1}(r,t)$ we can compute its discrete space Fourier transform to obtain the intermediate self-scattering-function $F_{s1}(k,t)$,

$$F_{s1}(k,t) = -G_{s1}(0,t) - (-1)^k G_{s1}(L/2,t) + 2\sum_{r=0}^{L/2} G_{s1}(r,t)\cos q_k r, \qquad \text{where} \quad q_k = \frac{2\pi}{L}k \quad , \quad (10)$$

and normalize it for $t = 0$. Note that, due to the sum rule $\sum_{r=0}^{L/2} G_{s1}(r,t) \equiv 0$, we have $F_{s1}(0,t) \equiv 0$ for all times t.

In Fig. 3 we show the typical behavior of $F_{s1}(k,t)$ for low, intermediate, and high densities. We emphasize that all curves shown represent equilibrium averages. (The fact that at high densities the curves do not decay to zero in the time window of our calculations does not indicate that the runs are of insufficient length to achieve equilibrium at high densities. Equilibrium initial states for the runs are trivial to obtain at all densities for this model.) We recognize that the smaller the value of k (i.e., the longer the wavelength), the slower the correlators relax. This can be understood by remembering the hydrodynamic relation [22]

$$\lim_{q_k \ll 1, t \gg 1} F_s(k,t) \propto \exp(-Dq_k^2 t) \quad . \quad (11)$$

We also observe that at high densities correlators for large values of k cluster and lie on a master curve. This master curve is well approximated by normalizing the space Fourier transform of the function given by $G_{s1}(r,t)\delta_{r,0}$, where δ is the Kronecker delta. Thus at high densities most of the relaxation behavior of the correlators can be described by the relaxation behavior of $G_{s1}(0,t)$.

In Fig. 4 we have plotted the correlators for small, intermediate and large values of k and for all densities investigated. We recognize that the correlators do not show the "two-step" relaxation behavior often found in glassy materials even at high densities, i.e., the correlators do not decay on a relatively short time scale to a plateau value [whose height is given by the nonergodicity parameter f, see Eq. (5)], stay in the vicinity of this plateau for some time, and then go over to the α-relaxation regime. Instead, in our model the correlators stay close to one for a time span that increases rapidly with increasing density. This absence of a plateau is not inconsistent with MCT, as can be seen from the following argument. When a particle in a real fluid is temporarily caged by its surroundings, it can nevertheless vibrate or "rattle" in its cage. The rattling motion does not by itself lead to diffusion but it will cause the correlator to relax to its plateau value. In our model almost all caged particles are completely immobile until their cages fall apart. The absence of rattling means that the value of the plateau is unity or very close to it. Thus the regime of the a power law [see Eq. (6)] would be very difficult or impossible to observe [3]. A similar behavior has been found in the relaxation behavior for one type of particle

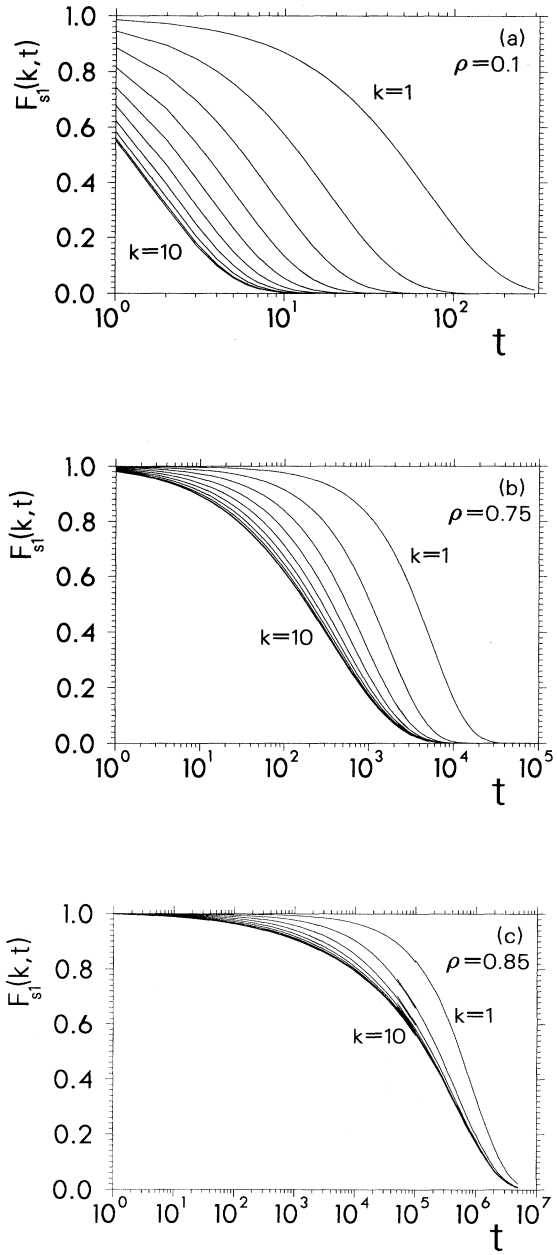

FIG. 3. Intermediate self-scattering-function $F_{s1}(k,t)$ for $k = 1, 2, \ldots, 10$ for $L = 20$ and various densities. (a) $\rho = 0.1$, (b) $\rho = 0.75$, (c) $\rho = 0.85$.

in an investigation of a two component lattice gas [10].

Figure 4 also shows that the functional form of the correlators does not depend strongly on density, i.e., the time-density superposition principle (TDSP) seems to hold quite well. Thus it is reasonable to define a relaxation time τ to be the time such that $F_{s1}(k,\tau) = e^{-1}$. Since the TDSP seems to hold quite well the results presented below will not have a significant dependence on the exact nature of this definition.

In order to test how well the TDSP really holds we plot in Fig. 5(a) $F_{s1}(k,t)$ for all densities investigated and $k = 1$ versus the rescaled time $t/\tau(\rho)$. We see that for short times $[t/\tau(\rho) < 1]$ the TDSP is clearly violated. For long times the TDSP seems to hold reasonably well, which shows that $\tau(\rho)$ is a good measure for the relaxation times of the correlators. We will postpone the discussion of the dependence of τ on the density until the last part of this subsection and concentrate now on the long-time behavior of the correlators.

Figure 5(b) shows the long-time behavior of $F_{s1}(k,t)$ for $k = 1$ and all densities investigated. We see that for low and intermediate densities ($\rho < 0.8$) the TDSP holds extremely well. We found that the master curve is an exponential for all times. For higher densities the correlators gradually deviate from this master curve. However, even for the highest density the deviation from the master curve is only about a factor of 2. The functional form of the correlators at high density and long times will be discussed later.

In the discussion of Fig. 4 we mentioned that the value of the nonergodicity parameter must be very close to one and that therefore the observation of the a power law is difficult. However, we still should be able to detect the von Schweidler law, i.e., the deviation of the correlator from this plateau. We therefore tried to fit the short-time behavior of the correlator with a power law of the form $F_{s1}(k,t) = f - Bt^b$. In Fig. 6 we plot $f - F_{s1}(k,t)$ versus t in a double logarithmic way. Thus in the time region where the von Schweidler law holds the curves are straight lines. We can see that at low densities this time

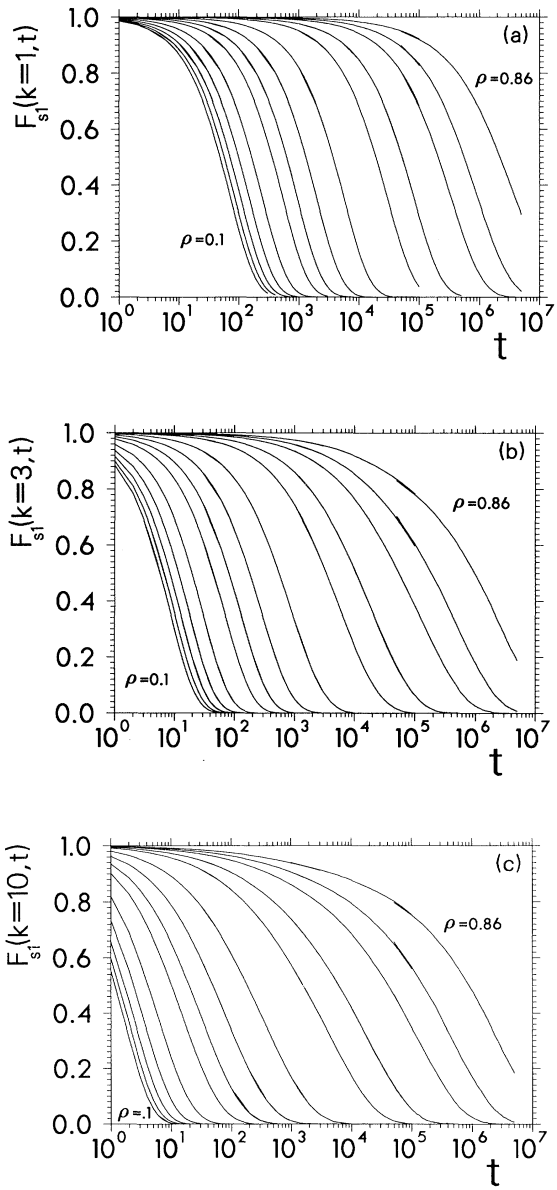

FIG. 4. Intermediate self-scattering-function $F_{s1}(k,t)$ for $L = 20$ and all densities investigated (see caption of Fig. 1). (a) $k = 1$, (b) $k = 3$, (c) $k = 10$.

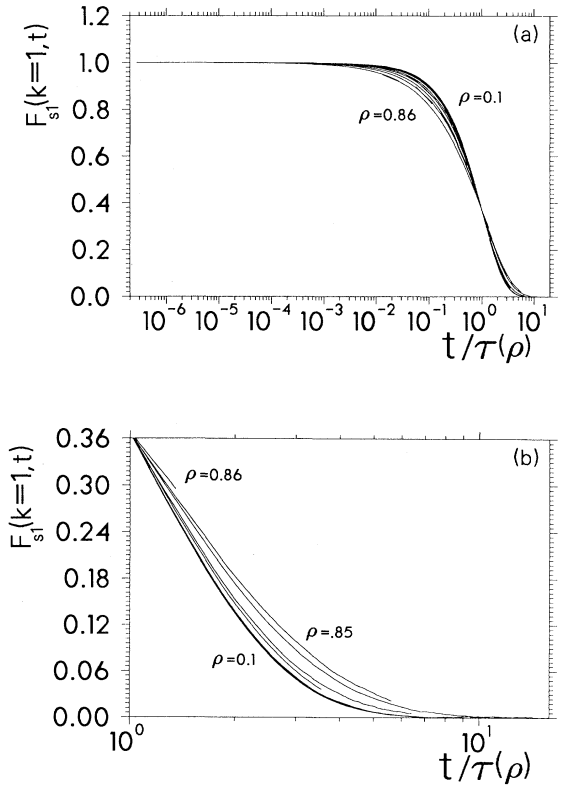

FIG. 5. (a) Intermediate self-scattering-function $F_{s1}(k,t)$ for $L = 20$, $k = 1$ and all densities investigated (see caption of Fig. 1) versus rescaled time $t/\tau(\rho)$. (b) Same as in (a) for long times.

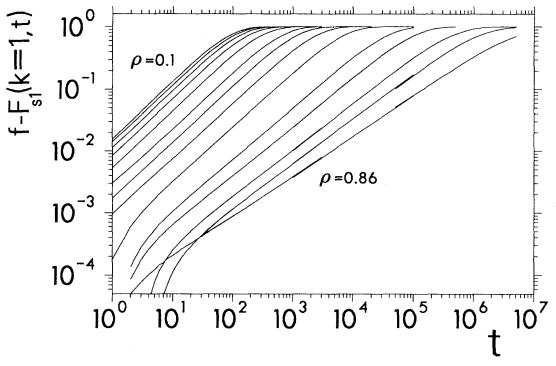

FIG. 6. Test for the presence of the von Schweidler law in $F_{s1}(k,t)$ for $k = 1$ and $L = 20$ and all densities investigated (see caption of Fig. 1). Straight line sections of the curves show where the law holds.

range is only about an order of magnitude and we therefore do not ascribe much significance to the fit. However, when the density is increased this range quickly increases to several orders of magnitude and the fit is thus much more convincing. The values of f we find from the fits are all very close to one (to within 10^{-3}) but no definitive statement can be made about the dependence of f on the density. From Fig. 6 we can recognize the clear trend that the slopes of those parts of the curves where the von Schweidler law holds decrease with increasing density. This means that exponent b is not independent of density, which is in contradiction with MCT. From Fig. 6 we see that the von Schweidler law holds only for times for which the correlator has not decayed below 0.8 [i.e., where $1 - F_{s1}(1,t) < 0.2$].

For long times the functional form of the correlator is given by a KWW law. To demonstrate the quality of such a fit, we plot in Fig. 7 $-\log_{10}[F_{s1}(k,t)/A(\rho)]$ versus time t in a double logarithmic way [A is the amplitude of the KWW law, see Eq. (4)]. Thus straight lines correspond to KWW behavior. We find that for small and intermediate densities the slopes, which are given by the KWW exponent β, are one, i.e., the decay is exponential.

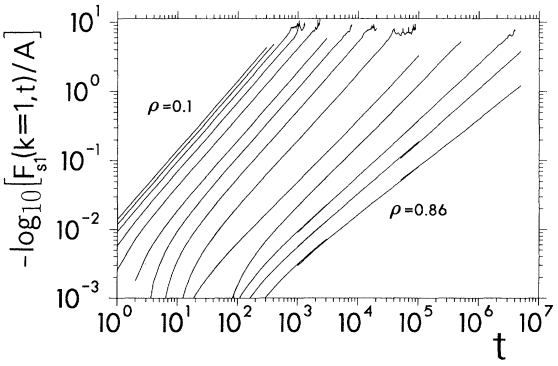

FIG. 7. Test for the presence of the KWW law in $F_{s1}(k,t)$ for $k = 1$ and $L = 20$ and all densities investigated (see caption of Fig. 1). Straight line sections of the curves show where the law holds.

This is in accordance with our discussion in connection with Fig. 5. For higher densities ($\rho > 0.75$) the slopes start to decrease monotonically. Thus β depends on density and the TDSP does not hold. Also note that the power-law behavior of $F_{s1}(k,t)$ at short times (Fig. 6) is *not* the power-law which is obtained by making a Taylor expansion of the KWW function at short times. If this would be the case the KWW fits would be valid also for short times and not break down at high densities the way it is observed in Fig. 7.

So far we have mainly discussed the relaxation behavior of correlators for a small value of k. However, the main focus of MCT are correlators which probe the system on the length scale of typical interparticle distances, i.e., for large values of k. We therefore also investigated the behavior for such correlators and proceed now to present our findings.

In Fig. 8(a) we show $F_{s1}(k,t)$ for $k = 10$, $L = 20$ for all densities investigated versus the rescaled time $t/\tau(\rho)$. We see that for low densities (curves on the left) the TDSP is clearly violated. However, for high densities ($\rho > 0.75$) the correlators start to cluster and form a master curve. In order to show how well these correlators fall onto the master curve we show them again in Fig. 8(b) on an extended time scale. We see that the TDSP holds for

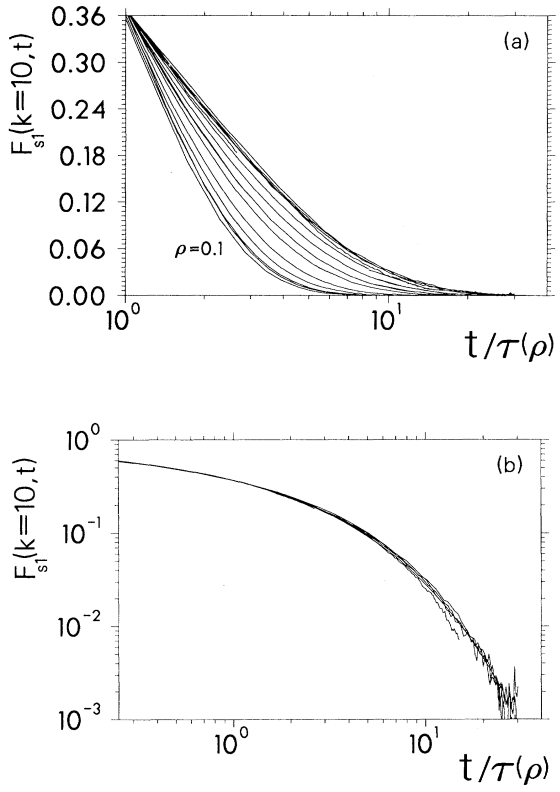

FIG. 8. (a) Long-time behavior of the intermediate self-scattering-function $F_{s1}(k,t)$ for $k = 10$ and $L = 20$ and all densities investigated (see caption of Fig. 1) versus rescaled time $t/\tau(\rho)$. (b) Same correlators as in (a) but only for $\rho > 0.75$. Also included is the result of a KWW fit for $0.3 \leq t/\tau(\rho) \leq 25$.

about two orders of magnitude in time. Note that the relaxation times $\tau(\rho)$ for this density range vary by a factor of 500 and that therefore the existence of a master curve is highly nontrivial. We have tried to fit the master curve with a KWW law and the best fit is included in the figure as well. For the time range of the fit we chose $0.3 \leq t/\tau(\rho) \leq 25$ and found the Kohlrausch exponent β to be 0.628. If we make KWW fits to the individual curves we find that the quality of the fit is reasonable but not very good. We demonstrate this in Fig. 9 where we plot, analogously to Fig. 7, $-\log_{10}[F_{s1}(k,t)/A(\rho)]$ versus time t. We recognize that for high densities ($\rho \geq 0.8$) the curves are parallel but not perfect straight lines even for long times. Thus the TDSP holds but the functional form is only approximately a KWW law. From this plot we can, however, see that the low- and intermediate-density behavior of the correlators is in fact given by a KWW law. The corresponding exponent is one only for very low densities and decreases monotonically when the density is increased up to intermediate densities.

We also tested whether the short-time behavior of these correlators can be fitted by a von Schweidler law too and found that this functional form is not able to fit the data well. Thus this prediction of MCT does not seem to hold. Instead a fit with the function

$$F_{s1}(k=10,t) = A - B[\ln(t/\tau)]^{\alpha} \tag{12}$$

gave very satisfactory fits over several orders of magnitude of time for $\rho \geq 0.65$. However, since we do not have a theory which suggests the use of this functional form we cannot ascribe any physical significance to the fit.

Previous work has shown that the time Fourier transform of correlation functions can be useful for detecting certain types of relaxation behaviors (see, e.g., [10]). We therefore computed the time Fourier transform for selected correlators but, apart from the power law which we already found in the time domain, no new features were discovered.

The results presented so far in this section dealt with the time correlation function as defined in Eq. (9). In addition we have also investigated the autocorrelation function $G_{s2}(r,t)$ which is defined as

$$G_{s2}(r,t) = \frac{1}{3N}\sum_{\alpha}\sum_{i=1}^{N}\langle\delta(\mathbf{r}_i(t)-\mathbf{r}_i(0)-r\hat{\mathbf{e}}_{\alpha})\rangle - \frac{1}{L^3} \quad . \tag{13}$$

Here $\hat{\mathbf{e}}_{\alpha}$ stands for the unit vector of the lattice pointing in direction α. Thus the sum on the right hand side is the (unnormalized) probability of finding a particle at time t on one of the axes defined by the location of the particle at time zero and at a distance of r lattice spacings from its location at time zero. Proceeding now analogously as in the case of $G_{s1}(r,t)$ we can define $F_{s2}(k,t)$. Comparing the relaxation behavior of $G_{s1}(r,t)$ and $G_{s2}(r,t)$ we found that the two correlators behave very similarly at high densities and large values of k except that $F_{s2}(k,t)$ shows a much weaker dependence on k than $F_{s1}(k,t)$. Thus for these densities and wave vectors we have the same results as in the case of $F_{s1}(k,t)$.

Finally we consider the behavior of the relaxation time τ as a function of density. We tried to fit $\tau(\rho)$ with a power law and in Fig. 10 we present the data for $L = 20$ on a log-log plot. Thus a power-law behavior would yield a straight line. Figure 10(a) shows the relaxation times obtained from $F_{s1}(k,t)$ and Fig. 10(b) those for $F_{s2}(k,t)$. The different curves correspond to different values of k. Note that the dependence of τ on k is much weaker for $F_{s2}(k,t)$ than for $F_{s1}(k,t)$, which is in accord with the

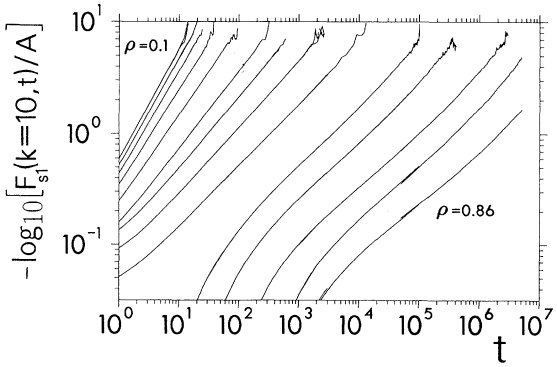

FIG. 9. Test for the presence of the KWW law in $F_{s1}(k,t)$ for $k = 10$ and $L = 20$ and all densities investigated (see caption of Fig. 1). Straight line sections of the curves show where the law holds.

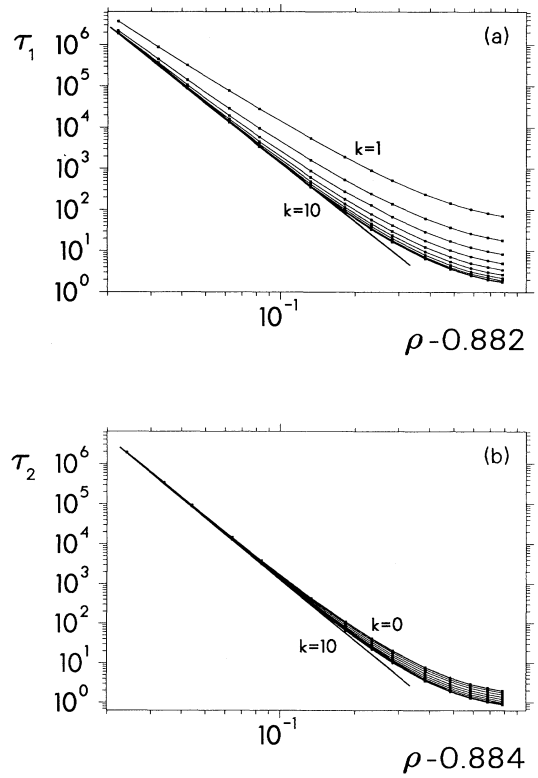

FIG. 10. Relaxation times τ for (a) $F_{s1}(k,t)$ and (b) $F_{s2}(k,t)$ for $L = 20$ as a function of density. The different curves correspond to different values of k. Straight lines are power-law fits.

previously stated fact that the dependence of F_{s2} on k is much weaker than that of F_{s1}.

When doing the fit we concentrated on the relaxation times for large values of k. We found that for high densities the $\tau(\rho)$ can be fitted well by a power-law behavior (straight lines in Fig. 10). It is remarkable that the critical densities we obtain from the fits (0.882 for τ_1 and 0.884 for τ_2) are almost identical for the two kinds of correlators. Also the two critical exponents are very close (4.9 for τ_1 and 5.1 for τ_2). This reflects the fact that the long-time behavior of the two correlators is so similar. For τ_1 and $L = 10$ and 14 we obtained $\rho_c = 0.869$ and 0.878, respectively, and critical exponents 4.1 and 4.6. Thus we find a small dependence on system size for the critical density and the exponent. The observation that the critical density for the relaxation times shows a stronger system size dependence than the one found for the diffusion constant might be due to the way we define a relaxation time. Since the time density superposition principle does not hold perfectly a different definition might lead to a slightly different critical behavior and to a different dependence on system size.

We also found that the relaxation time τ for small values of k can be fitted well by a power-law behavior. The critical densities are all very close to the ones we found for large values of k (for both, τ_1 and τ_2). However, the critical exponents are not the same for the two quantities. For τ_2 they are close to the ones we found for large values of k and for τ_1 they are all around 3.2, i.e., very close to the critical exponent we found for the diffusion constant. Thus it seems that correlators which are associated with conserved quantities (the diffusion constant and F_{s1} for small values of k) have the same value of the critical exponent whereas correlators which do not have this property (F_{s1} for large values of k and F_{s2} for all values of k) have a different kind of exponent. The same observation was also made for a different kind of lattice gas [10] thus showing that this behavior is not unique to the model studied here.

In summary we can say that all these values for the critical density are close to the size-independent value of 0.881 for the critical density for diffusion. These data strongly suggest that the dynamical transition exists in the thermodynamic limit at a density of about 0.88, well below the maximum density of the system.

V. DISCUSSION OF FINITE-SIZE EFFECTS

In the preceding section, we presented evidence, from simulations at densities of 0.86 and less, that indicated the presence of a dynamical singularity for this model at a critical density of about 0.88. Since the calculations were necessarily done for small finite-sized systems we should be concerned with whether the singularity will be present in the thermodynamic limit. For the range of system sizes studied we observed a small system size dependence of the values of the diffusion constant as a function of density, only a very slight size dependence of the value of the critical density determined from the density dependence of the relaxation time, and no size dependence of the value of the critical density determined from the density dependence of the diffusion coefficients. Obviously it is impossible to prove from simulations alone the existence of a dynamical singularity in the thermodynamic limit. However, consider the following summary of the important observations: (1) the two ways of estimating the critical density led to consistent results with either no, or only a slight, system size dependence; (2) the critical (i.e., power-law) dependence of the diffusion constant on density was observed for over three decades of variation of its value; (3) the critical dependence of the relaxation times on density was observed for almost four decades of its variation; and (4) the critical dependence was observed for a range of densities that extended to within 2% of the critical density of 0.88. This type of evidence would ordinarily be sufficient to establish the credibility of the assertion that a dynamical singularity of some sort is taking place in this system at densities below the filled lattice density of 1. One cause for concern, however, is that one can show that the dynamics of this model shows finite-size effects at densities well below 1 even for systems that are much larger than those we report on here.

To see this consider the possibility that a system subject to periodic boundary conditions might contain the following structure—a linear array of particles that extends from one side of the system to the other, that makes contact with its periodic image, and whose cross section is a two by two array of particles. If the length of the cubic system is L, then this structure would contain $4L$ particles. Each of the particles in the structure would have four nearest neighbor particles in the structure. As a result, under the dynamics of the model, none of the $4L$ particles would ever be able to move. For this type of immobility to occur, it is important that the structure spanning the entire system makes contact with its own image. A similar structure of $4n$ particles for $n < L$ would not have such an immobility since the particles at the ends of the structure would have less than four neighboring particles in the structure, which could allow them to move, thereby freeing particles further along the structure for subsequent motion. One can imagine more elaborate structures with the same immobility, containing, for example, two or more such sets of $4L$ immobile particles, arrayed parallel to or perpendicular to one another, with "bridges" of particles connecting them. A bridge of $4n$ particles (i.e., four adjacent lines of particles in a two by two array) each of whose ends made sufficient contact with one of the set of particles that span the system would also be completely immobile.

A set of particles with these characteristics will be called a "backbone." The possible presence of a backbone has two important consequences: The first is that the relaxation behavior of a system at a given density with a backbone differs from the behavior of a system at the same density but without a backbone. The fact that some particles are completely immobile means that they contribute nothing to the mean-squared displacement of particles and hence this will lead to a lowering of the calculated diffusion constant. Moreover, the particles that are mobile will be somewhat constrained in their motion by the presence of the static backbone, and this is

also likely to decrease the diffusion constant. The second consequence is that if, at a given density, an appreciable fraction of the states of the system have a backbone, then the dynamics of the model is not ergodic. Because the model obeys a detailed balance condition, a system without a backbone could never develop one and a system with a backbone could never destroy it.

Thus backbones can interfere with the relaxation properties of a system and cause dynamical artifacts and anomalies. The question arises of whether the formation of such backbones can be the cause of the apparent dynamical singularity of the system at a density of 0.88. Closely related to this is the question of whether the presence of backbones is a finite-size effect and whether the dynamical singularity at 0.88 is a finite-size effect.

The presence of a backbone in a state of the model system can be detected by applying the following algorithm to the state: Remove each particle that satisfies both of the following conditions: (1) the particle has three or fewer neighbors; and (2) adjacent to the particle is a vacant site that has four or fewer neighboring particles. We continue this process until all particles have been removed or until all the remaining particles fail to satisfy one or both of these conditions. The particles that remain are the backbone of the original state.

For various system sizes and densities, we have applied this algorithm to a random sample of initial states to determine the ensemble average of p, the probability that a particle is a member of the backbone, as a function of density and system size. The results are presented in Fig. 11. These curves were obtained by averaging over from 1000 (for $L = 50$) to 100 000 (for $L = 10$) initial configurations. We also determined P, the probability that a system has a backbone, as a function of density and system size and plot it in Fig. 12.

From these two figures, we can draw the following conclusions. (1) The presence of a backbone is clearly a finite-size effect for densities of 0.88 and lower. Both p and P decrease systematically as system size is increased at fixed density, and for a density of 0.88 the backbone is of negligible importance for systems as small as $L = 40$. (2) For the largest system size we investigated ($L = 20$), backbones could have no appreciable effect on the calculated dynamical properties over the range of densities

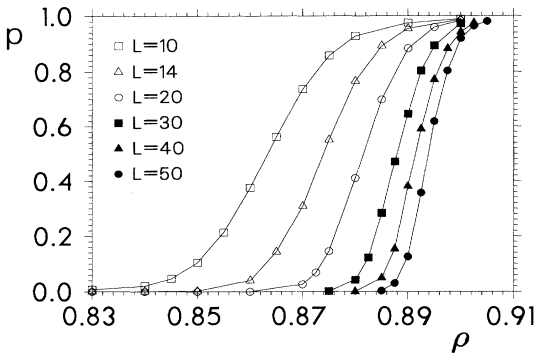

FIG. 11. Probability p that a particle is a member of the backbone versus density ρ for different system sizes L.

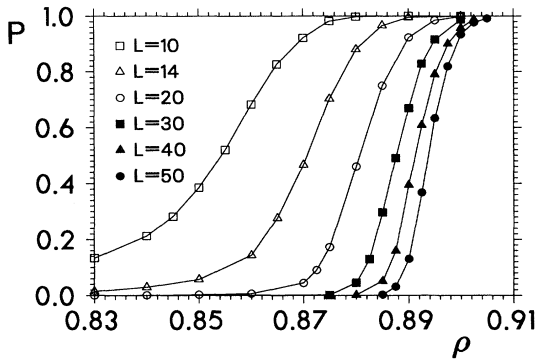

FIG. 12. Probability P that a system has a backbone versus density ρ for different system sizes L.

investigated (0.86 and lower). For example, at a density of 0.86, the fraction of $L = 20$ states that have a backbone is 0.007, and the probability that a particle is part of a backbone is 8×10^{-5}. (3) The three system sizes we studied had significantly different average fractions of particles in the backbone for the density range indicated. This presumably accounts for the small system size dependence to the diffusion constants as seen in Fig. 2. Despite this, the density at the singularity, which was inferred from the density dependence of the diffusion constant and relaxation time, was remarkably insensitive to the system size. The net effect of these observations is to confirm that the dynamical anomaly at a density of 0.88 is not an artifact due to the presence of backbones.

The presence of a backbone for our problem is closely related to the presence of a percolating cluster in what is known as the "bootstrap percolation" problem. This problem has been studied by various authors in various connections [23,24] and the results have recently been reviewed by Adler [25]. The bootstrap percolation problem considers a lattice whose sites are occupied with probability ρ. The algorithm for the version of the bootstrap percolation problem that is closely related to our problem, i.e., for a three dimensional simple-cubic lattice, is very similar to the one we defined above to identify the backbone. It can be stated as follows: Given a state of the system, remove each particle that has three or fewer neighbors. We continue this process until all particles have been removed or until all the remaining particles fail to satisfy this condition. The particles that remain, if any, form a cluster that percolates across the periodic cell and makes contact with its own image.

The conditions for removing a particle in the bootstrap percolation problem are similar to but less stringent than those for our problem. As a result, for any starting state the infinite cluster of the bootstrap problem will always be a part of the backbone for our problem. By means of computer simulations we have found that the two percolation problems have similar properties but that percolating clusters become significant at a lower density for our model than for the bootstrap problem (for a given system size). For the bootstrap problem we can define a critical density $\rho_c^{(b)}(L)$ as the density at which half the systems have a percolating cluster. For a cubic lattice in three di-

mensions, it has been found [24] that $\lim_{L\to\infty} \rho_c^{(b)}(L) = 1$ but that the convergence of $\rho_c^{(b)}(L)$ to this value is extremely slow, i.e.,

$$1 - \rho_c^{(b)}(L) = O(1/\ln[\ln(L)]). \tag{14}$$

We would expect a similar behavior for our problem, confirming that the presence of a backbone is a finite-size effect. However, although the convergence to the infinite system limit for our model cannot be faster than the one for the bootstrap model [Eq. (14)], our empirical results, namely, that for the largest system the fractions of the particles in the backbone is very small, show that the presence of backbones cannot be an explanation of the anomalous behavior we have observed.

In order to investigate the importance of the dynamics of a single particle for the relaxation behavior of the whole system, we computed M, the mean number of directions a particle can move, as a function of density for $L = 10$, 14, and 20. In Fig. 13 we plot M versus $1 - \rho$ in a double logarithmic way. The plot shows that at high densities we find a power-law behavior with a critical density of unity (solid line). Contrary to the results presented in the two previous figures we do not find any significant dependence of M on system size L. This can be understood by realizing that M depends only on the local environment of the particles and not on structures which are so large that they span the whole system and which therefore are sensitive to the system size. We also recognize that $M(\rho)$ is featureless. Apart from $\rho = 1$ we do not find any density which would indicate a drastic change in the dynamics of the individual particles. This shows that the singular behavior reported in the preceding section cannot be attributed to a singular behavior of the motion of the individual particles since it is observed at densities below 1. Thus the singularity must be a cooperative effect.

VI. SUMMARY AND CONCLUSIONS

The model investigated in this work is a simple lattice gas with, except for a hard core, no interactions between the particles. The nontrivial part of the system is its dynamics. This dynamics is constructed so that the motion of a particle from one site to an adjacent site is prevented if the adjacent site is already occupied or if one of the two sites is surrounded by too many neighboring particles. These restrictions on particle motion are such that (i) a particle can become temporarily trapped by a cage of neighbors; (ii) the system is ergodic at low density; and (iii) the system becomes increasingly sluggish at higher density. Thus this model has the physical features associated with the "cage effect" in high-density liquids. Moreover, there is nothing in the dynamics that is suggestive of activated processes. The model has the very advantageous feature for computer simulations that it is trivial to generate equilibrium states to be used as starting points for runs to calculate time correlation functions. A random placement of particles on the lattice at the desired density, with no two particles on the same site, is a typical equilibrium configuration. No equilibration is necessary. This greatly facilitates the investigation of *equilibrium* properties of the system at high densities.

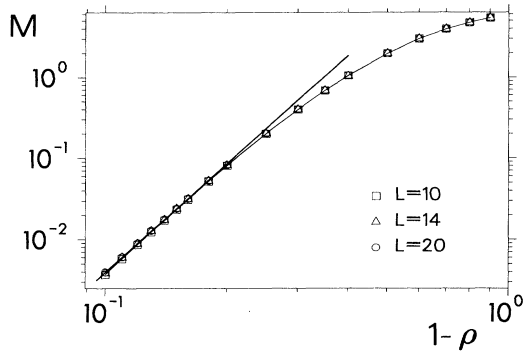

FIG. 13. Mean number of directions a particle can move, M, versus $1 - \rho$ for $L = 10$, 14, and 20. The straight line is a power-law fit with critical density 1.

Despite its simplicity the system shows a remarkably complex relaxation behavior that qualitatively matches the relaxation behavior found in real glassy materials. This and the above mentioned properties make it therefore a highly interesting model for testing the applicability of the version of MCT in which activated hopping processes are neglected.

We found that the diffusion constant seems to go to zero at a density well below that of the filled lattice and that this behavior can be described well by a power law. Hence, this prediction of MCT seems to be fulfilled for our model. We found that the critical density does *not* depend on the size of the system, which gives evidence that the vanishing of the diffusion constant has nothing to do with the presence of the nonergodic backbone discussed in Sec. V.

We have investigated the dynamical behavior of two types of relaxation functions: $F_{s1}(k,t)$ and $F_{s2}(k,t)$. Our main findings are the following: (i) For small values of k the short-time behavior of $F_{s1}(k,t)$ shows a von Schweidler law time dependence. However, the exponents depend on density, which is in contradiction with MCT. Also, we do not find the von Schweidler behavior for large values of k in $F_{s1}(k,t)$ nor for *any* value of k in $F_{s2}(k,t)$. (ii) The time-density superposition principle does not seem to hold for $F_{s1}(k,t)$ for small values of k and high densities. However, it seems to work well for large values of k and high densities and also for $F_{s2}(k,t)$ for all values of k at high densities. (iii) The form of the master curves of $F_{s1}(k,t)$ at high densities and large values of k and of $F_{s2}(k,t)$ for high densities and all values of k are only approximately described by a KWW law since small but systematic deviations are observed. (iv) The relaxation times τ show a power-law divergence at high densities.

From our findings we can see that only surprisingly few predictions of MCT hold for our system. Among the deviations from the predicted behavior, the most striking are the absence of the von Schweidler law in $F_{s1}(k,t)$ and $F_{s2}(k,t)$ for large values of k and the non-KWW behavior for these correlators. The fact that the dynamics of our system seems to contain quite a few features that

makes it a physically reasonable model for a glass made us expect that MCT would fare better than it actually does. Note that the highest densities we investigated correspond to an $|\epsilon|$ of about 0.02. Thus we performed the simulations in a density region in which we expected the predictions of MCT to hold, and it is improbable that a too large value of $|\epsilon|$ is the reason for the partial failure of MCT to describe our results. Also, the presence of nonequilibrium phenomena, always a potential source for problems in numerical simulations of glassy materials, can be completely ruled out. Thus we have to conclude that MCT does not seem to be able to describe this kind of model. This is surprising since our investigation of a related model showed much closer, although not perfect, agreement with the predictions of theory [10]. At the moment it is not clear to us what the essential properties of the dynamics are that are needed in order for the relaxation behavior of the system to be consistent with the predictions of MCT.

The apparent vanishing of the diffusion coefficient occurs at a density of 0.881. Therefore it would be very interesting to study the dynamics at densities of 0.881 and higher to provide additional tests of the existence of the transition and to characterize the behavior in the nonergodic regime. Because of the finite-size effects discussed above, simulations at a density of 0.881 would have to be performed on much larger systems than those we have investigated. Inspection of Fig. 11 shows that $L = 40$, with approximately 56 000 particles, would probably be big enough. The investigation of even slightly higher densities would require much larger systems. Moreover, the time ranges needed to obtain useful information from such studies at these densities would be much larger than those we have simulated in the present work.

Finally we note that with minor modifications, this model could be converted to one that includes moves that restore ergodicity and thereby play the role ascribed to activated processes in the mode-coupling theory. This could be done by randomly choosing between two different kinds of dynamics at each time step. The first kind is the one presented in this work. The second kind is that one chooses a particle and a direction at random and tries to move the chosen particle by one lattice spacing in the chosen direction. If the target vertex is occupied nothing is moved (but we advance the clock) and if it is empty we move the particle to it (and advance the clock). It is clear that this second kind of dynamics is ergodic. Let us define the probability that we have chosen this second kind of dynamics as δ. Thus $1-\delta$ is the probability that we chose the first kind of dynamics. If δ is nonzero the dynamics of the system will be ergodic for all densities. However, if δ is very small the effect of the second type of dynamics on the overall dynamics will be noticeable only for very long-times. The short- and intermediate-time behavior will be the same as reported in this work. Thus by varying δ one would be able to study the effects of the hopping processes as a function of their frequency and investigate how the presence of hopping processes leads to the smearing out of the sharp ergodic to nonergodic transition that is found in the absence of activated hopping processes.

ACKNOWLEDGMENTS

We would like to thank S. J. Pitts for a careful reading of the manuscript. Part of this work was supported by the Swiss National Science Foundation, and by National Science Foundation Grant No. CHE89-18841. We made use of computer resources provided under NSF Grant No. CHE88-21737.

[1] U. Bengtzelius, W. Götze, and A. Sjölander, J. Phys. C **17**, 5915 (1984); E. Leutheusser, Phys. Rev. A **29**, 2765 (1984).

[2] T. R. Kirkpatrick, Phys. Rev. A **31**, 939 (1985); S. P. Das, G. F. Mazenko, S. Ramaswamy, and J. J. Toner, Phys. Rev. Lett. **54**, 118 (1985); W. Götze, Z. Phys. B **60**, 195 (1985); U. Bengtzelius, Phys. Rev. A **34**, 5059 (1986); S. P. Das and G. F. Mazenko, *ibid.* **34**, 2265 (1986); H. De Raedt and W. Götze, J. Phys. C **19**, 2607 (1986); L. Sjögren, Phys. Rev. A **33**, 1254 (1986); W. Götze and L. Sjögren, J. Phys. C **20**, 879 (1987); U. Krieger and J. Bosse, Phys. Rev. Lett. **59**, 1601 (1987); K. H. Michel, Z. Phys. B **68**, 259 (1987); W. Götze and R. Haussmann, *ibid.* **72**, 403 (1988); J.-L. Barrat, W. Götze, and A. Latz, J. Phys. Condens. Matter **1**, 7163 (1989); W. Götze and L. Sjögren, *ibid.* **1**, 4183 (1989); W. Götze and L. Sjögren, J. Phys. Condens. Matter **1**, 4203 (1989); S. P. Das, Phys. Rev. A **42**, 6116 (1990); M. Fuchs, W. Götze, I. Hofacker, and A. Latz, J. Phys. Condens. Matter **3**, 5047 (1991); G. Szamel and H. Löwen, Phys. Rev. A **44**, 8215 (1991); J. S. Thakur and J. Bosse, *ibid.* **43**, 4378 (1991); **43**, 4388 (1991); M. Fuchs, I. Hofacker, and A. Latz, *ibid.* **45**, 898 (1992); B. Kim, *ibid.* **46**, 1992 (1992); S. P. Das, J. Chem. Phys. **98**, 3328 (1993).

[3] G. Buchalla, U. Dersch, W. Götze, and L. Sjögren, J. Phys. C **21**, 4239 (1988).

[4] W. Götze and L. Sjögren, Z. Phys. B **65**, 415 (1987); J. Phys. C **21** 3407 (1988); L. Sjögren, Z. Phys. B **79**, 5 (1990); L. Sjögren and W. Götze, J. Non-Cryst. Solids **131-133**, 153 (1991); M. Fuchs, W. Götze, S. Hildebrand, and A. Latz, J. Phys. Condens. Matter **4**, 7709 (1992).

[5] L. Sjögren, J. Phys. Condens. Matter **3**, 5023 (1991).

[6] L. Sjögren, Phys. Rev. A **22**, 2866 (1980), and references therein.

[7] G. Wahnström and L. Sjögren, J. Phys. C **15**, 401 (1982).

[8] F. Fujara and W. Petry, Europhys. Lett. **4**, 921 (1987); F. Mezei, W. Knaak, and B. Farago, Phys. Rev. Lett. **58**, 571 (1987); P. N. Pusey and W. van Megen, *ibid.* **59**, 2083 (1987); B. Frick, D. Richter, W. Petry, and U. Buchenau, Z. Phys. B **70**, 73 (1988); W. Knaak, F. Mezei, and B. Farago, Europhys. Lett. **7**, 529 (1988); D. Richter, B. Frick, and B. Farago, Phys. Rev. Lett. **61**,

2465 (1988); J.-L. Barrat, J.-N. Roux, and J.-P. Hansen, Chem. Phys. **149**, 197 (1990); W. Doster, S. Cusack, and W. Petry, Phys. Rev. Lett. **65**, 1080 (1990); M. Fuchs, W. Götze, and A. Latz, Chem. Phys. **149**, 185 (1990); J.-L. Barrat and J.N. Roux, J. Non-Cryst. Solids **131-133**, 255 (1991); S. Flach, J. Siewert, R. Siems, and J. Schreiber, J. Phys. Condens. Matter **3**, 7061 (1991); W. Kob and R. Schilling, *ibid.* **3**, 9195 (1991); L. J. Lewis, Phys. Rev. B **44**, 4245 (1991); W. Petry, E. Bartsch, F. Fujara, M. Kiebel, H. Sillescu, and B. Farago, Z. Phys. B **83**, 175 (1991); W. Götze and L. Sjögren, Phys. Rev. A **43**, 5442 (1991); W. van Megen and P. N. Pusey, *ibid.* **43**, 5429 (1991); W. van Megen, S. M. Underwood, and P. N. Pusey, Phys. Rev. Lett. **67**, 1586 (1991); G. Wahnström, Phys. Rev. A **44**, 3752 (1991); S. Flach and J. Siewert, J. Phys. Condens. Matter **4**, L363 (1992); M. Fuchs, W. Götze, S. Hildebrand, and A. Latz, Z. Phys. B **87**, 43 (1992); M. Elmroth, L. Börjesson, and L. M. Torell, Phys. Rev. Lett. **68**, 79 (1992); S. Flach and J. Siewert, Phys. Rev. B **47**, 14 910 (1993); C. Dreyfus, M. J. Lebon, H. Z. Cummins, J. Toulouse, B. Bonello, and R. M. Pick, Phys. Rev. Lett. **69**, 3666 (1992); G. Li, W. M. Du, X. K. Chen, H. Z. Cummins, and N. J. Tao, Phys. Rev A **45**, 3867 (1992); G. Li, W. M. Du, A. Sakai, and H. Z. Cummins, *ibid.* **46**, 3343 (1992); M. Kiebel, E. Bartsch, O. Debus, F. Fujara, W. Petry, H. Sillescu, Phys. Rev. B **45**, 10301 (1992); O. T. Valls and G. F. Mazenko, Phys. Rev. A **46**, 7756 (1992); Phys. Rev. Lett. **70**, 2766 (1993); W. van Megen and S. M. Underwood, Phys. Rev. E **47**, 248 (1993); S. K. Lai and H. C. Chen, J. Phys. Condens. Matter **5**, 4325 (1993); X. C. Zeng, D. Kivelson, and G. Tarjus (unpublished); H. Z. Cummins, W.M. Du, M. Fuchs, W. Götze, A. Latz, G. Li, and N.J. Tao, Phys. Rev. E **47**, 4223 (1993); G. Li, W. M. Du, J. Hernandez, and H. Z. Cummins, *ibid.* **48**, 1192 (1993).

[9] E. Bartsch, F. Fujara, M. Kiebel, H. Sillescu, and W. Petry, Ber. Bunsenges. Phys. Chem. **93**, 1252 (1989); L. Börjesson and W. S. Howells, J. Non-Cryst. Solids **131-133**, 53 (1991); B. Frick, B. Farago, and D. Richter, Phys. Rev. Lett. **64**, 2921 (1990); E. Bartsch, M. Antonietti, W. Schupp, and H. Sillescu, J. Chem. Phys. **97**, 3950 (1992).

[10] W. Kob and H. C. Andersen, Phys. Rev. E **47**, 3281 (1993).

[11] G. H. Fredrickson and H. C. Andersen, Phys. Rev. Lett. **53**, 1244 (1984); J. Chem. Phys. **83**, 5822 (1985).

[12] G. H. Fredrickson and S. A. Brawer, J. Chem. Phys. **84**, 3351 (1986).

[13] W. Ertel, K. Froböse, and J. Jäckle, J. Chem. Phys. **88**, 5027 (1988).

[14] K. Froböse, J. Stat. Phys. **55**, 1285 (1989).

[15] J. Jäckle, K. Froböse, and D. Knödler, J. Stat. Phys. **63**, 249 (1991).

[16] J. Reiter, F. Mauch, and J. Jäckle, Physica A **184**, 458 (1992).

[17] R. H. Schonmann, J. Stat. Phys. **58**, 1239 (1990).

[18] J. Jäckle and D. Sappelt, Physica A **192**, 691 (1993).

[19] W. Götze, in *Liquids, Freezing and the Glass Transition*, Les Houches Session LI, 1989, edited by J. P. Hansen, D. Levesque, and J. Zinn-Justin (North-Holland, Amsterdam, 1991); W. Götze and L. Sjögren, Rep. Prog. Phys. **55**, 241 (1992); R. Schilling, in *Disorder Effects on Relaxational Processes*, edited by R. Richert and A. Blumen (Springer, Berlin, 1994).

[20] Ajay and R. G. Palmer, J. Phys. A **23**, 2139 (1990).

[21] See, e.g., the comment by P. W. Anderson on p. 287, Ann. N. Y. Acad. Sci. **484** (1986).

[22] J.-P. Hansen and I. R. McDonald, *Theory of Simple Liquids* (Academic, London, 1986).

[23] J. Chalupa, P. L. Leath, and G. R. Reich, J. Phys. C **12**, L31 (1979); P. M. Kogut and P. L. Leath, *ibid.* **14**, 3187 (1981); P. M. Kogut, J. Chalupa, and P. L. Leath, *ibid.* **15**, 6689 (1982); M. Aizenman and J. L. Lebowitz, J. Phys. A **21**, 3801 (1988); S. S. Manna, D. Stauffer, and D. W. Heermann, *ibid.* **162**, 20 (1989); M. Sahimi and T. S. Ray, J. Phys. I **1**, 685 (1991).

[24] A. C. D. van Enter, J. Adler, and J. A. M. S. Duarte, J. Stat. Phys. **60**, 323 (1990).

[25] J. Adler, Physica A **171**, 453 (1991).